

A relationship between d_{104} value and composition in the calcite-disordered dolomite solid-solution series

FANGFU ZHANG, HUIFANG XU,* HIROMI KONISHI, AND ERIC E. RODEN

NASA Astrobiology Institute, Department of Geoscience, University of Wisconsin–Madison, Madison, Wisconsin 53706, U.S.A.

ABSTRACT

X-ray diffraction has been widely used in analyzing Ca-Mg carbonates. Compositions of biogenic and inorganic (Ca,Mg)CO₃ crystals are often calculated by comparing their d_{104} values with published empirical curves. However, previous studies suggested that these curves do not apply to very high-Mg calcite and disordered dolomite. Based on synthesized high-Mg calcite and disordered dolomite, a new empirical curve between values of magnesian calcite d_{104} and MgCO₃ content in the calcite-disordered dolomite solid-solution series is constructed. This new curve is consistent with the significant cell parameter changes accompanying the Mg-Ca cation disorder in dolomite, and it can help the characterization of the MgCO₃ content of both natural and synthetic magnesian calcite and disordered dolomite, especially for the mineral mixtures that are not suitable for other analysis methods.

Keywords: High-magnesian calcite, d_{104} , calcite, disordered dolomite, solid solution, Mg-Ca ordering in dolomite

INTRODUCTION

X-ray diffraction (XRD) is a long-established technique for compositional determination in solid-solution series. Differences in ionic sizes between substituting and host cations lead to systematic variations in unit-cell parameters and interplanar d -spacings that can be measured using XRD. This approach has been widely used in analyzing rhombohedral Ca-Mg carbonates. For example, compositions of biogenic and inorganic (Ca,Mg)CO₃ crystals are often calculated by comparing measured d_{104} value with published determinative curves (Milliman et al. 1971; Bischoff et al. 1983; Falini et al. 1996; Raz et al. 2000). There are at least five empirical curves currently in the literature (Chave 1952; Goldsmith et al. 1955, 1961; Goldsmith and Graf 1958; Milliman et al. 1971; Bischoff et al. 1983). Determinative curves based on synthetic magnesian calcite crystals (Goldsmith and Graf 1958; Goldsmith et al. 1961; Milliman et al. 1971) are probably the most widely used. However, the validity of these curves has been disputed, especially for high-Mg content crystals (Reeder and Sheppard 1984). Previous working approximation assumes that d -spacings should lie on a straight line connecting the respective values for pure calcite and ideal stoichiometric dolomite. However, there is no systematic investigation of well-characterized natural dolomites that support this approximation (Reeder and Sheppard 1984).

Another deficiency with these curves came from the samples used in these studies. Samples used in early studies with compositions close to stoichiometric dolomite are ordered dolomite. Ca-Mg disordering in dolomite causes expansion in the unit-cell dimensions (Goldsmith et al. 1961; Reeder and Wenk 1983; Antao et al. 2004; Carmichael and Ferry 2008). In other words,

the cation disordering between Ca and Mg will increase the d -spacings of dolomite. Previously published empirical curves are not applicable to very high-magnesian calcite (VHMC) and disordered dolomite. It is true that magnesian calcite with more than just a few mole percents MgCO₃ are metastable or unstable except at high temperatures (above the solvus line) according to the phase diagram (Anovitz and Essene 1987). However, high-magnesian calcite and disordered dolomite do occur in natural environments. For example, many organisms form skeletons composed of high-Mg calcite with greater than 10 mol% MgCO₃ content (Raz et al. 2000) and some as high as 40 mol% (Schroede et al. 1969). VHMC with variable MgCO₃ content, disordered dolomite, and proto-dolomite occur in cold-seep areas (Stakes et al. 1999). An empirical curve comparing d_{104} to MgCO₃ content for disordered counterparts would be therefore useful to study VHMC and disordered dolomite skeletal particles and cements. Based on this premise, a new empirical curve is constructed based on synthesized high-magnesian calcite (HMC) and disordered dolomite. The new relationship can help quantify the MgCO₃ content in both natural and synthetic VHMC and disordered dolomite, especially for mineral mixtures that are not suitable for other analysis methods, e.g., atomic absorption, ICP-AES, and electron microprobe.

EXPERIMENTAL METHODS

Synthesis of HMC and disordered dolomite in sulfide/acetate/methane-bearing solutions

Chemicals with low dielectric constants can promote the Mg incorporation into calcite and thus promote high-magnesian calcite and disordered dolomite formation (Oomori and Kitano 1987; Falini et al. 1996). Our results also show that aqueous sulfide, acetate, and methane that have very low dielectric constants can catalyze HMC and disordered dolomite formation. Pyrite surface may offer heterogeneous nucleation sites to HMC and disordered dolomite. HMC and disordered dolomite were precipitated by mixing NaHCO₃+Na₂S (with or without pyrite)/sodium acetate

* E-mail: hfxu@geology.wisc.edu

($C_2H_3NaO_2$) solution and $CaCl_2+MgCl_2$ solution together. A solution of 60 mL 10 mM $CaCl_2$ + 50 mM $MgCl_2$ was infused into 60 mL 50 mM $NaHCO_3$ + Na_2S (with or without pyrite)/ $C_2H_3NaO_2$. Different concentrations of Na_2S and sodium acetate were used. Water bath was used when conducting experiments at slightly high temperatures (Table 1). All the solutions were bubbled with N_2 to eliminate O_2 before experiments. Fresh pyrite powders were prepared from fresh pyrite hand specimens and passed through a 50 μm sized sieve to get pyrite powders.

A Parr-type acid digestion vessel was used to dissolve significant methane in the solutions. A container with 250 mL 42.5 mM $NaHCO_3$ + 7.5 mM Na_2CO_3 solution was put inside the digestion vessel. Then a smaller container with 150 mL 50 mM $MgCl_2$ + 10 mM $CaCl_2$ solution was put into the container with 250 mL $NaHCO_3$ + Na_2CO_3 solution. This was followed by the infusion of methane gas into the digestion vessel, and the digestion vessel was then put into an oven that was set to 50 °C for 24 h. The final pressure was adjusted to ~5 bar. Then the digestion vessel was tilted in the oven so that the two solutions inside can mix together. Finally, the digestion vessel was vigorously shaken to make sure that two solutions could mix thoroughly. After mixing, the precipitates were collected for further analyses.

X-ray diffraction (XRD) analysis

X-ray diffraction analyses were carried out using a Scintag Pad V diffractometer (CuK α radiation) and Rigaku Rapid II X-ray diffraction system with a 2D image plate (MoK α radiation). The Scintag diffractometer was operated at 45 kV, 40 mA with CuK α radiation, and used a 2 mm divergence slit, 4 mm incident scatter slit, 1 mm diffracted beam scatter slit, and 0.5 mm receiving slit. All the synthesized samples analyzed by using the Scintag diffractometer were deposited on a low-background quartz plate. Samples analyzed by using Rapid II diffraction system were put in thin wall glass capillary tubes. Diffraction data were collected on an image-plate detector. The two-dimensional images were then integrated to produce conventional 2 θ -I patterns using Rigaku's 2DP software.

The Rietveld method was used to obtain cell parameters of our synthetic carbonates. The Rietveld method, in contrast to the profile-fitting procedure of integrated peak intensities, employs the entire powder diffraction pattern, thereby overcoming the problem of peak overlap. In this method, each data point (2 θ step) is considered as an observation, which thus allows the maximum amount of information to be extracted from the pattern (Rietveld 1967, 1969). During the refinement procedure, structural parameters, background coefficients, and profile parameters are varied in a least-squares procedure until the calculated powder profile, based on the structure model, best matches the observed pattern (Rietveld 1967, 1969; Post and Bish 1989). MDI's Jade (version 9) Whole Pattern Fitting (WPF) program was used for the Rietveld refinement analyses. Atom positions of a magnesian calcite was taken from the structural refinement result of $Ca_{0.9}Mg_{0.1}CO_3$ (Althoff 1977) for an initial disordered dolomite, and Mg/Ca ratios were constrained to be those obtained by EDS analysis. $R\bar{3}c$ was chosen as the space group for disordered dolomite.

Scanning electron microscope (SEM), transmission electron microscopy (TEM), and selected-area electron diffraction (SAED) analyses

SEM samples were prepared by dispersing powders on sample stages and then lightly carbon-coated. SEM observation was performed using a Hitachi S3400

SEM equipped with energy-dispersive X-ray spectroscopy (EDS) capabilities to determine the solid-phase composition.

TEM and SAED measurements were carried out using a Philips CM 200UT microscope [with a spherical aberration coefficient (Cs) of 0.5 mm and a point-to-point resolution of 0.19 nm] equipped with an EDS analyzer (NORAN Voyager), and operated at 200 kV.

Analysis of Mg composition in HMC and disordered dolomite

X-ray energy-dispersive spectroscopy (EDS) in the Philips CM 200UT microscope was used to measure $MgCO_3$ content more precisely from crystal to crystal. X-ray microanalysis of thin specimens in the TEM offers nano-scale information on the chemistry of materials. While the overall concept remains the same, thin film areas of TEM samples are thin enough to be beam transparent, so the ionization volume formed by a focused probe is much smaller and, therefore, there is much less electron scattering (Cliff and Lorimer 1972, 1975; Lorimer et al. 1972; Lippmann 1973; Lorimer and Champness 1973; Joy et al. 1986; Williams and Carter 1996). High electron-beam energies (100–400 keV) utilized in the analytical TEM also reduce beam scattering. Thus, the corrections normally associated with the analysis of thick SEM specimens do not apply to thin TEM specimens (Cliff and Lorimer 1972, 1975; Lorimer et al. 1972; Lippmann 1973; Lorimer and Champness 1973). Consequently, quantification may be performed by using a simple ratio technique first developed by Cliff and Lorimer (1972). Cliff and Lorimer (1972) observed that peak intensities are proportional to concentration and specimen thickness. They removed the effects of variable specimen thickness by taking ratios of intensities for elemental peaks and introduced a "k-factor" to relate the intensity ratio to concentration ratio $C_A/C_B = k_{AB} * I_A/I_B$, where I_A = peak intensity of element A and C_A is concentration in wt% or mass fraction. Each pair of elements requires a different k-factor that depends on detector efficiency, ionization cross-section, and fluorescence yield of the two elements concerned.

In this case, Cliff-Lorimer factors for Mg and Ca were obtained using a well-characterized dolomite standard from Delight, Baltimore (49.43 mol% $CaCO_3$, 50.48 mol% $MgCO_3$, and 0.09 mol% $FeCO_3$, by electron microprobe analysis). The k-factors calculated from several EDS spectra varied from 1.147 to 1.184. For an EDS spectra that has 50 mol% $MgCO_3$, the error should be within 1.6 mol% for analyzing dolomite. The relative error would be expected to be larger for samples with lower $MgCO_3$ content. Thus, all the composition values calculated with EDS method were estimated to be within 2 mol% of error. SEM studies showed that HMC or disordered dolomite mostly occur as spherical clusters composed of a great number of nano-crystals. To make sure that the compositions of the core of the spherical clusters would be collected, a small amount of each sample was thoroughly crushed between two glass slides or in a small agate mortar with a few drops of ethanol. A drop of the resulting suspension was placed on a holey-carbon film supported by a TEM Cu grid and air-dried. All the areas for EDS spectra collection were characterized using SAED to confirm they were pure HMC or disordered dolomite. At least 20 EDS spectra were collected from different crystals grains for each synthesized sample. To ensure the accuracy of every measurement, an acquisition time was long enough to accumulate at least 10000 counts for Ca and Mg peaks (Williams and Carter 1996). To eliminate the effect of X-ray absorption, the beam was always put at the thin edge of the sample to ensure that the illumination area is thin enough for electrons to penetrate and only

TABLE 1. Compositions of synthetic HMC and disordered dolomite

| d_{104} (Å) measured* | d_{104} (Å) based on refinement† | $MgCO_3$ % based on XRD‡ | $MgCO_3$ % based on EDSS | $MgCO_3$ % range based on EDS | Synthesis method# |
|-------------------------|------------------------------------|--------------------------|--------------------------|-------------------------------|---|
| 2.988 | 2.9899 | 16.3% | – | – | Sodium acetate, room temperature (5 mM) |
| 2.972 | – | 22.5% | – | – | Sodium sulfide, room temperature (5 mM) |
| 2.957 | 2.9588 | 27.8% | 28.7% | 18.2%~36.6% | Sodium sulfide, room temperature (7.5 mM) |
| 2.953 | – | 29.6% | 32.2% | 25.8%~39.2% | Sodium sulfide, pyrite, room temperature (7.5 mM) |
| 2.947 | 2.9467 | 32.1% | 38.0% | 34.0%~43.1% | Methane, 50 °C |
| 2.943 | 2.9409 | 33.2% | 41.0% | 35.6%~48.5% | Sodium sulfide, 35 °C (7.5 mM) |
| 2.932 | 2.9326 | 36.8% | 45.2% | 36.2%~50.1% | Sodium sulfide, 45 °C (7.5 mM, final pH = 8.1) |
| 2.932 | – | 37.0% | 46.2% | 38.7%~54.0% | Sodium sulfide, 45 °C (7.5 mM, final pH = 9.4) |
| 2.912 | 2.9171 | 43.9% | 54.1% | 47.8%~58.4% | Sodium sulfide, 60 °C (7.5 mM, final pH = 8.5) |

* d_{104} values based on XRD patterns.

† d_{104} values are from refinement.

‡ Molar content of $MgCO_3$ based on the Goldsmith et al. (1961) curve.

§ Average $MgCO_3$ content based on TEM EDS data.

|| $MgCO_3$ content variation based on TEM EDS data.

See Experimental Methods for details.

spectra in which the height of $OK\alpha$ peak is close to that of $CaK\alpha$ peaks were used for further quantification. Samples that have EDS spectra with obvious Na peaks are excluded from this study. Thermo Electron's NORAN System SIX software was used to quantify the collected EDS spectra.

For HMC with <28 mol%, the differences between average compositions based on Goldsmith et al. (1961) curve and X-ray EDS method are very small (<1 mol%). Thus the composition of these HMC with <20 mol% of $MgCO_3$ can be simply obtained based on Goldsmith et al. (1961) curve.

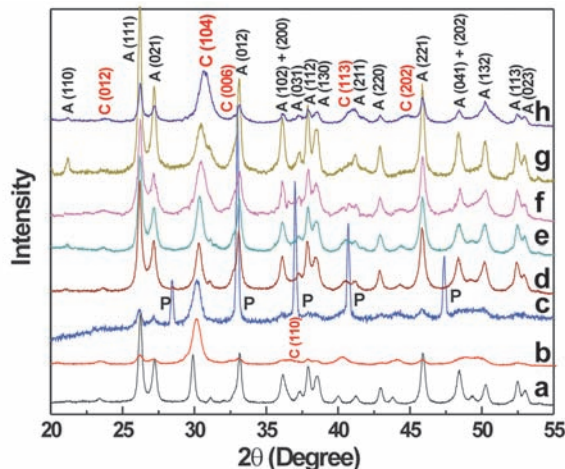


FIGURE 1. XRD patterns of synthesized HMC and disordered dolomite. Shaded area marks VHM or disordered dolomite (104) peaks. (a) Aragonite and VHM (16.3 mol% of $MgCO_3$) synthesized in sodium acetate-bearing solutions at 25 °C; (b) aragonite and VHM (28.7 mol% of $MgCO_3$) synthesized in sodium sulfide-bearing solutions at 25 °C; (c) aragonite and VHM (~ 32.2 mol% of $MgCO_3$) induced by sodium sulfide and pyrite (0.175 g); (d) aragonite and disordered dolomite (38.0 mol% of $MgCO_3$) synthesized in methane-bearing solutions; (e) aragonite and disordered dolomite (41.0 mol% of $MgCO_3$) synthesized in sodium sulfide-bearing solutions at 35 °C; (f) aragonite and disordered dolomite (45.2 mol% of $MgCO_3$) synthesized in sodium sulfide-bearing solutions at 45 °C; (g) aragonite and disordered dolomite (46.2 mol% of $MgCO_3$) synthesized in sodium sulfide-bearing solutions at 45 °C; (h) aragonite and disordered dolomite (54.1 mol% of $MgCO_3$) synthesized in sodium sulfide-bearing solutions at 60 °C. C = VHM or disordered dolomite; A = aragonite; P = pyrite. All the compositions are based on TEM X-ray EDS spectra. (Color online.)

RESULTS

XRD patterns of synthesized HMC and disordered dolomite are shown in Figure 1. Broadened X-ray diffraction peaks were noted for HMC and disordered dolomite. In general, the broad peaks can result from inhomogeneities in chemical composition and extremely fine crystal size (Bischoff et al. 1983). SEM and TEM studies showed that synthetic HMC or disordered dolomite mostly occur as spherical clusters that are composed of many nano-crystals with variable chemical composition (Figs. 2 and 3). Thus, nano-crystals of HMC and disordered dolomite crystals with variable $MgCO_3$ most likely resulted in the broadened XRD peaks in this case (Table 1; Fig. 2).

SAED patterns show that these nano-crystals were not at random orientations, but rather show low-angle grain boundaries between neighboring crystals (Fig. 3a). The [010] zone-axis fast Fourier transform (FFT) pattern does not show superlattice reflections that appear in the dolomite structure. If there is ordering between Mg and Ca, a set of reflections that are forbidden in calcite [010] zone-axis SAED patterns would appear in the dolomite [010] zone-axis SAED patterns. Thus the VHM and disordered dolomite were completely disordered, which were suitable for this study. The Ca-Mg ordering occurs when synthesized disordered dolomite was annealed at 300 °C for 140 h (Figs. 3c–3d). The superlattice reflections characterizing ordered dolomite structure appeared in diffraction pattern (Fig. 3c–3d). The d_{104} values did decrease with the cation ordering in disordered dolomite (Fig. 4).

The Rietveld refinements show good agreement between calculated diffraction patterns and observed XRD patterns (Fig. 5). The difference between d_{104} values from refinements and XRD patterns are generally <0.002 Å (Table 1). Selected refinement results are listed in the Appendix¹.

¹ Deposit item AM-10-053, Appendix Tables 1–6. Deposit items are available two ways: For a paper copy contact the Business Office of the Mineralogical Society of America (see inside front cover of recent issue) for price information. For an electronic copy visit the MSA web site at <http://www.minsocam.org>, go to the *American Mineralogist* Contents, find the table of contents for the specific volume/issue wanted, and then click on the deposit link there.

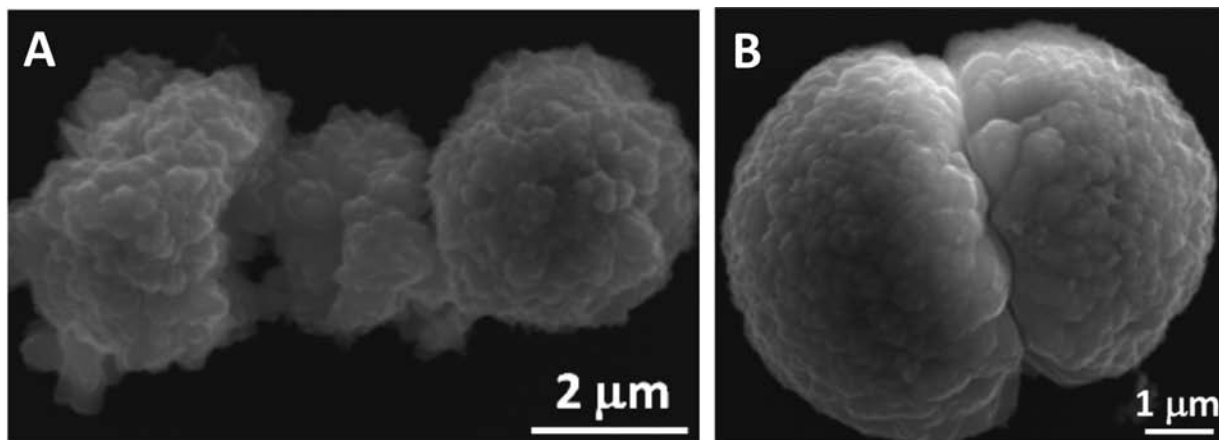


FIGURE 2. SEM images of the synthesized disordered dolomite. Notice that these spherical clusters are actually composed of nano-crystals stacking together. (a) SEM image of spherical clusters composed of disordered dolomite synthesized from a sulfide-bearing solution ($[Na_2S] = 7.5$ mM, $T = 45$ °C); (b) SEM image of a disordered dolomite dumbbell synthesized from methane-bearing solutions ($T = 50$ °C, ~ 5 bar of methane gas).

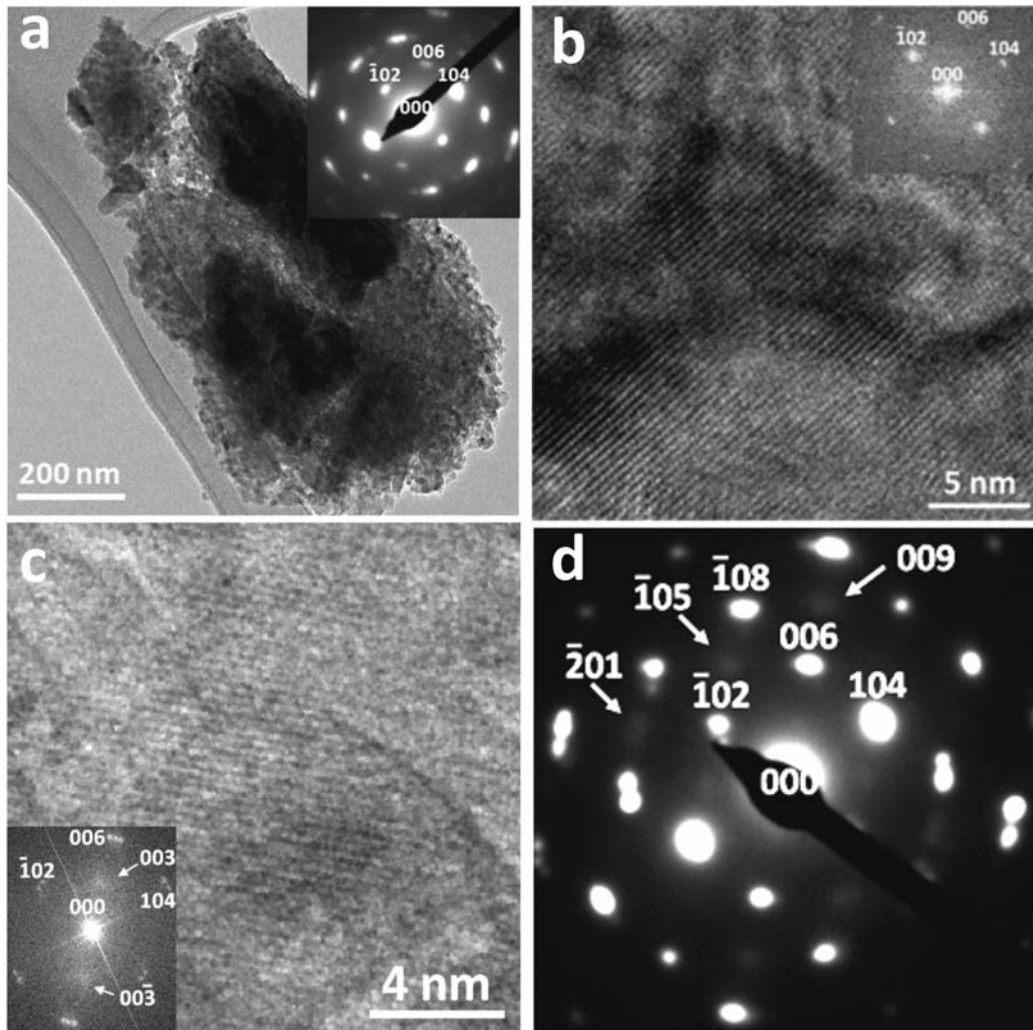


FIGURE 3. TEM study of disordered dolomite: (a) TEM image showing disordered dolomite nano-crystals (~50 mol% of MgCO_3). Inset is a [010] zone-axis SAED pattern, which shows that there was no Ca-Mg ordering and these nano-crystals are not at random orientations, but with low-angle grain boundaries. (b) HRTEM image of the disordered dolomite (~50 mol% of MgCO_3) with (006) lattice fringes, no (003) superlattice fringes. Inset is a [010] zone-axis FFT pattern showing no super-lattice reflections. (c) HRTEM image of the annealed dolomite showing (003) superlattice fringes that characterizing Ca-Mg order. Inset is a [010] zone-axis FFT pattern showing weak super-lattice reflections. (d) SAED pattern from the annealed dolomite. Arrows indicate weak super-lattice reflections like 003, 009, and $\bar{1}05$ characterizing Ca-Mg ordering.

DISCUSSION

Based on synthetic VHMC and disordered dolomite, new curves of d_{104} values and lattice constants a and c vs. the MgCO_3 content in the calcite-disordered dolomite solid-solution series were constructed (Figs. 6 and 7). The variation of d_{104} values and cell parameters with the MgCO_3 content do not display a linear relationship as that was proposed in previous works (Goldsmith and Graf 1958; Goldsmith et al. 1961). The difference between average compositions based on Goldsmith et al. (1961) curve and X-ray EDS method are very small (<1%) for those with <28 mol% of MgCO_3 content. The difference gets larger as the MgCO_3 content increases (Fig. 6; Table 1). For example, for a disordered dolomite with a d_{104} of 2.932 Å, obtained compositions directly from EDS analyses and measured from Goldsmith

et al. (1961) curve are 46.2 and 37.0 mol% of MgCO_3 contents, respectively (Table 1).

The Ca-Mg disordered dolomite structure results in the changes in unit-cell parameters (Goldsmith et al. 1961; Reeder and Wenk 1983; Antao et al. 2004). For complete disordered dolomite, Reeder and Wenk (1983) estimated a 0.07 Å change in c -dimension, which is about twice the value suggested by Goldsmith et al. (1961), and lattice constants of $a = 4.805$, $c = 16.071$ Å, which are significantly smaller than the values ($a = 4.8435$, $c = 16.320$ Å), we calculated based on our new curves (Fig. 7). Because completely disordered crystals could not be recovered owing to reordering during the quench, Reeder and Wenk (1983) estimated the cell parameters for complete disorder by extrapolation based on the assumption that a linear relation-

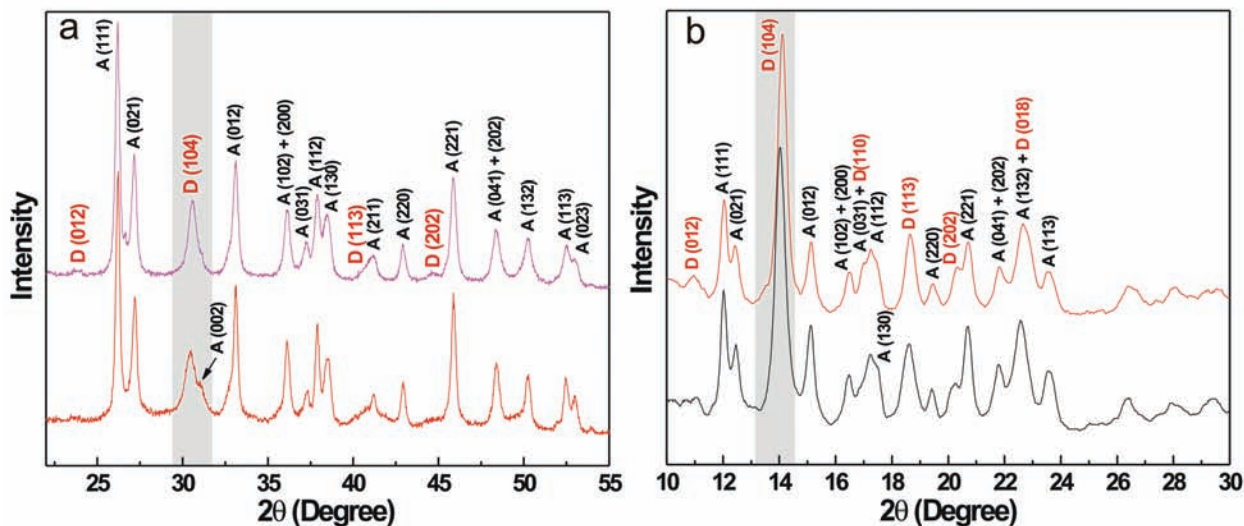


FIGURE 4. XRD patterns showing that the Ca-Mg order decreases the d -spacings of disordered dolomite. Shaded area marks VHMC or disordered dolomite (104) peaks. (a) (CuK α radiation) bottom pattern: aragonite and disordered dolomite (46.2 mol% of MgCO₃, d_{104} = 2.932 Å) synthesized in sodium sulfide-bearing solutions at 45 °C; top pattern: sample annealed at 300 °C for 140 h (d_{104} = 2.918 Å). Notice that aragonite (002) peak is clear in the bottom pattern. But after annealing, aragonite (002) is overlapped with the disordered dolomite (104) peak indicating the peak shift of the (104) diffraction. (b) (MoK α radiation) bottom pattern: aragonite and disordered dolomite (54.1 mol% of MgCO₃, d_{104} = 2.9171 Å) synthesized in sodium sulfide-bearing solutions at 60 °C; right-top pattern: sample in the bottom pattern annealed at 300 °C for 24 h (d_{104} = 2.891 Å) indicating the peak shift. D = dolomite; A = aragonite. All the compositions are based on TEM X-ray EDS spectra. (Color online.)

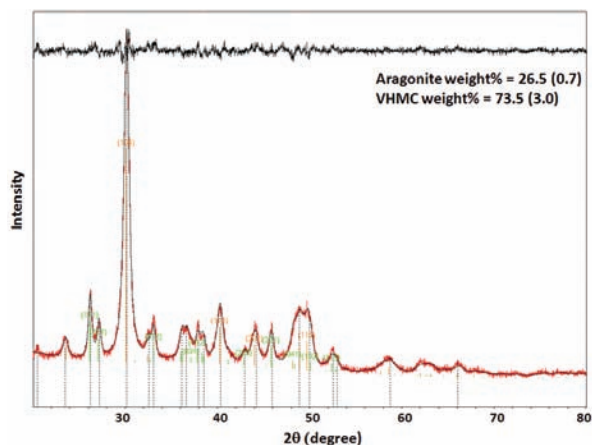


FIGURE 5. A typical Rietveld refinement result of synthetic VHMC and aragonite. The black curve on the top indicates residuals between the measured and calculated patterns. The two agreement factors of this refinement are weighted (R) value of 4.64% and expected value of 3.6%, respectively. (Color online.)

ship between cell parameters and degree of disorder. However, samples used in Reeder and Wenk (1983) experiments still had an order parameter larger than 0.7, which means that these samples were still well ordered. Thus, they pointed out that caution should be taken with their estimated cell parameters since considerable extrapolation was required and errors can be large. Our experimental data clearly demonstrate that the estimated cell parameters for disordered dolomite by Reeder and Wenk (1983) were underestimated (Fig. 7), which was also confirmed by recent studies (Antao et al. 2004). Using in situ synchrotron powder XRD at very high-pressure and Rietveld refinement method, Antao et al.

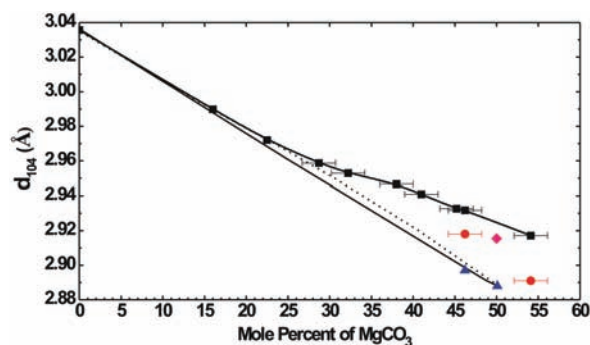


FIGURE 6. A new empirical curve between d_{104} values and composition in the calcite-disordered dolomite solid-solution series. Black squares are data from this study. The two blue triangles are from two ordered dolomite (46.2% MgCO₃, a = 4.819 Å, c = 16.097 Å; 50.1% MgCO₃, a = 4.813 Å, c = 16.023 Å), which are from Reeder and Sheppard (1984). The pink diamond is from sample close to completely ordered dolomite (order parameter = 0.12) (Antao et al. 2004). The two red circles indicate the weakly ordered dolomite with average compositions of 46.2 and 54.1% MgCO₃ by annealing the disordered dolomite at 300 °C for 140 and 24 h, respectively. The errors for compositions of samples with more than 28 mol% MgCO₃ are estimated to be within 2 mol%. The errors associated with d_{104} values which are calculated from the Rietveld refinement (see supporting materials) are within the size of the symbol. The straight solid line and dashed line are the idealized curve (Goldsmith and Graf 1958) and Goldsmith et al. (1961) curve. (Color online.)

(2004) calculated the lattice constants of a dolomite with an order parameter of 0.12, that is, a = 4.8072, c = 16.3354 Å (Table 2). The d_{104} value (2.915 Å) and unit-cell volume (326.92 Å³) for almost completely disordered dolomite calculated from Antao et al. (2004) are smaller than that of the present study (a d_{104} value of 2.9246 Å and unit-cell volume of 331.56 Å³, respectively,

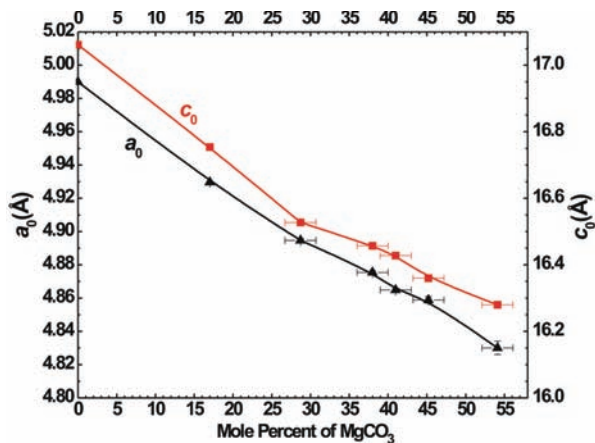


FIGURE 7. Diagram illustrating the relationship between a_0 , c_0 value, and composition in the calcite-disordered dolomite solid-solution series. The errors for compositions of samples with more than 28 mol% MgCO_3 are estimated to be within 2 mol%. The errors associated with a_0 and c_0 values are from the Rietveld refinement (see supporting materials), and are within the size of the symbol for most samples. a_0 = black triangles; c_0 = red squares. (Color online.)

see Table 2), which is reasonable considering that the crystals investigated in Antao et al. (2004) were under very high pressure (3 GPa). The mean (linear) compressibilities of the a and c axes of ordered dolomite are $1.922 \times 10^{-3}/\text{GPa}$ and $5.823 \times 10^{-3}/\text{GPa}$ (Ross and Reeder 1992). Assuming that the compressibilities of the a axes of ordered and disordered dolomite are similar, the disordered dolomite, if compressed at 3 GPa, should have similar a values with that of Antao et al. (2004). However, the disorder would definitely affect the compressibility of the c axis because compression along c is the net effect of compression of the CaO_6 and MgO_6 octahedra (Ross and Reeder 1992) and some MgO_6 octahedra, which are supposed to be heavily compressed in ordered dolomite, may only be slightly compressed due to the shielding of the larger CaO_6 octahedra in the same cation layers. Due to the lack of the compressibility of the c axis of disordered dolomite, we can offer no reasonable explanations to the discrepancy between the c values from Antao et al. (2004) and the present study. A complete study of the ordering kinetics of dolomite crystals with different compositions will be carried out in the future.

The new empirical curve can help the characterization of the MgCO_3 content of both natural and synthetic VHMC and disordered dolomite, especially for mineral mixtures not suitable

TABLE 2. Lattice parameters and cell volumes of disordered and ordered dolomite

| | a_0 (Å) | c_0 (Å) | V (Å ³) |
|------------------------------|-----------|-----------|-----------------------|
| Ordered dolomite (1 atm)* | 4.8072 | 16.0048 | 320.31 |
| Ordered dolomite (3 GPa)† | 4.7795 | 15.7252 | 311.09 |
| Disordered dolomite (1 atm)‡ | 4.8435 | 16.320 | 331.56 |
| Disordered dolomite (3 GPa)§ | 4.8072 | 16.3354 | 326.92 |

* From Antao et al. (2004).

† Calculated lattice parameters based on Antao et al. (2004) and Ross and Reeder (1992).

‡ From the present study.

§ From Antao et al. (2004).

for other analysis methods, e.g., atomic absorption, ICP-AES, and electron microprobe. It is noteworthy that sometimes a small amount of minor phases, e.g., clay-like brucite $[\text{Mg}(\text{OH})_2]$, in the mixture can be invisible in XRD patterns. And if these minor phases were not recognized and the mineral mixtures were treated as a pure phase, analysis methods like atomic absorption, ICP-AES, and electron microprobe could produce erroneous results due to the contribution from minor phases, e.g., brucite. Thus, this new empirical would provide an accurate and straightforward way to study chemical compositions of HMC and disordered dolomite in mixture samples.

ACKNOWLEDGMENTS

We thank Abby Kavner and the other anonymous reviewer, and the associate editor, Darrell Henry, for their great comments and suggestions. We also want to thank John Fournelle for providing the dolomite standard and Nita Sahai for constructive discussions. This work is supported by NASA Astrobiology Institute (N07-5489), NSF (EAR-0810150, EAR-095800), and U.S. Department of Energy (DE-SC0001929). Zhang also thanks Department of Geoscience, University of Wisconsin-Madison and ExxonMobil for 2008 Summer Research Grant, and Geological Society of America for 2009 Graduate Research Grant.

REFERENCE CITED

- Althoff, P.L. (1977) Structural refinements of dolomite and a magnesian calcite and implications for dolomite formation in marine-environment. *American Mineralogist*, 62, 772–783.
- Anovitz, L.M. and Essene, E.J. (1987) Phase-equilibria in the system CaCO_3 - MgCO_3 - FeCO_3 . *Journal of Petrology*, 28, 389–414.
- Antao, S.M., Mulder, W.H., Hassan, I., Crichton, W.A., and Parise, J.B. (2004) Cation disorder in dolomite, $\text{CaMg}(\text{CO}_3)_2$, and its influence on the aragonite + magnesite \leftrightarrow dolomite reaction boundary. *American Mineralogist*, 89, 1142–1147.
- Bischoff, W.D., Bishop, F.C., and Mackenzie, F.T. (1983) Biogenically produced magnesian calcite inhomogeneities in chemical and physical-properties comparison with synthetic phases. *American Mineralogist*, 68, 1183–1188.
- Carmichael, S.K. and Ferry, A.M. (2008) Formation of replacement dolomite in the Latemar carbonate buildup, dolomite, Northern Italy: Part 2. Origin of the dolomitization fluid and the amount and duration of fluid flow. *American Journal of Science*, 308, 885–904.
- Chave, K.E. (1952) A solid solution between calcite and dolomite. *The Journal of Geology*, 60, 190–192.
- Cliff, G. and Lorimer, G.W. (1972) Quantitative analysis of thin metal foils using EMMA-4—The ratio technique. *Proceedings of the 5th European Congress on Electron Microscopy*, p. 140–141. Institute of Physics, London.
- (1975) The quantitative analysis of thin specimens. *Journal of Microscopy*, 103, 203–207.
- Falini, G., Gazzano, M., and Ripamonti, A. (1996) Magnesium calcite crystallization from water-alcohol mixtures. *Chemical Communications*, 1037–1038, DOI: 10.1039/CC9960001037.
- Goldsmith, J.R. and Graf, D.L. (1958) Relation between lattice constants and composition of the Ca-Mg carbonate. *American Mineralogist*, 43, 84–101.
- Goldsmith, J.R., Graf, D.L., and Joensuu, O. (1955) The occurrence of magnesian calcite in nature. *Geochimica et Cosmochimica Acta*, 7, 212–230.
- Goldsmith, J.R., Graf, D.L., and Heard, H.C. (1961) Lattice constants of the calcium-magnesium carbonates. *American Mineralogist*, 46, 453–459.
- Joy, D.C., Romig, A.D.J., and Goldstein, J.I. (1986) *Principles of Analytical Electron Microscopy*. Plenum Press, New York.
- Lippmann, F. (1973) *Sedimentary Carbonate Minerals*, 228 p. Springer, New York.
- Lorimer, G.W. and Champness, P.E. (1973) Combined electron-microscopy and analysis of an orthopyroxene. *American Mineralogist*, 58, 243–248.
- Lorimer, G.W., Nasir, M.J., Nicholson, R.B., Nutall, K., Ward, D.E., and Webb, J.R. (1972) The use of an analytical electron microscope (EMMA-4) to investigate solute concentrations in thin metal foils. In G. Thomas, Ed., *Electron Microscopy and Structure of Materials*, p. 222–234. University of California Press, Berkeley.
- Milliman, J.D., Gastner, M., and Muller, J. (1971) Utilization of magnesium in coralline algae. *Geological Society of America Bulletin*, 82, 573–580.
- Oomori, T. and Kitano, Y. (1987) Synthesis of protodolomite from sea-water containing dioxane. *Geochemical Journal*, 21, 59–65.
- Post, J.E. and Bish, D.L. (1989) Rietveld refinement of crystal structures using powder X-ray diffraction data. In D.L. Bish and J.E. Post, Eds., *Modern Powder Diffraction*, 20, p. 277–308. Reviews in Mineralogy, Mineralogical Society of America, Chantilly, Virginia.

- Raz, S., Weiner, S., and Addadi, L. (2000) Formation of high-magnesian calcites via an amorphous precursor phase: Possible biological implications. *Advanced Materials*, 12, 38–42.
- Reeder, R.J. and Sheppard, C.E. (1984) Variation of lattice-parameters in some sedimentary dolomites. *American Mineralogist*, 69, 520–527.
- Reeder, R.J. and Wenk, H.R. (1983) Structure refinements of some thermally disordered dolomites. *American Mineralogist*, 68, 769–776.
- Rietveld, H.M. (1967) Line profiles of neutron powder-diffraction peaks for structure refinement. *Acta Crystallographica*, 22, 151–152.
- (1969) A profile refinement method for nuclear and magnetic structures. *Journal of Applied Crystallography*, 2, 65–71.
- Ross, N.L. and Reeder, R.J. (1992) High-pressure structural study of dolomite and ankerite. *American Mineralogist*, 77, 412–421.
- Schroede, J.H., Dwornik, E.J., and Papike, J.J. (1969) Primary protodolomite in echinoid skeletons. *Geological Society of America Bulletin*, 80, 1613–1616.
- Stakes, D.S., Orange, D., Paduan, J.B., Salamy, K.A., and Maher, N. (1999) Cold-seeps and authigenic carbonate formation in Monterey Bay, California. *Marine Geology*, 159, 93–109.
- Williams, D.B. and Carter, C.B. (1996) *Transmission Electron Microscopy: A Textbook for Materials Science*. Plenum Press, New York.

MANUSCRIPT RECEIVED OCTOBER 2, 2009

MANUSCRIPT ACCEPTED JUNE 15, 2010

MANUSCRIPT HANDLED BY DARRELL HENRY